TU Delft

Delft University of Technology

Document Version
Final published version

Licence
CC BY

Citation (APA)
Imron, M. F., van den Berg, L., Hendriks, A., Lindeboom, R. E. F., & de Kreuk, M. (2026). Evaluating the role of iron dosing in sludge reduction in a sequencing batch reactor integrated with an anaerobic side-stream reactor. *Journal of Environmental Chemical Engineering*, *14*(6), Article 124966. https://doi.org/10.1016/j.jece.2026.124966

Important note
To cite this publication, please use the final published version (if applicable).
Please check the document version above.

Copyright
In case the licence states “Dutch Copyright Act (Article 25fa)”, this publication was made available Green Open Access via the TU Delft Institutional Repository pursuant to Dutch Copyright Act (Article 25fa, the Taverne amendment). This provision does not affect copyright ownership.
Unless copyright is transferred by contract or statute, it remains with the copyright holder.

Sharing and reuse
Other than for strictly personal use, it is not permitted to download, forward or distribute the text or part of it, without the consent of the author(s) and/or copyright holder(s), unless the work is under an open content license such as Creative Commons.

Takedown policy
Please contact us and provide details if you believe this document breaches copyrights.
We will remove access to the work immediately and investigate your claim.

This work is downloaded from Delft University of Technology.

Journal of Environmental Chemical Engineering 14 (2026) 124966

Contents lists available at ScienceDirect

Journal of Environmental Chemical Engineering

journal homepage: www.elsevier.com/locate/jece

Evaluating the role of iron dosing in sludge reduction in a sequencing batch reactor integrated with an anaerobic side-stream reactor

Muhammad Fauzul Imron [a,b,*], Lenno van den Berg [c], Alexander Hendriks [c], Ralph E.F. Lindeboom [b], Merle de Kreuk [b]

[a] Study Program of Environmental Engineering, Department of Biology, Faculty of Science and Technology, Universitas Airlangga, Kampus C UNAIR, Jalan Mulyorejo, Surabaya, 60115, Indonesia
[b] Department of Water Management, Faculty of Civil Engineering and Geosciences, Delft University of Technology, Stevinweg 1, Delft, 2628CN, the Netherlands
[c] Haskoning, Laan 1914 no 35, Amersfoort, 3818EX, the Netherlands

ARTICLE INFO

Keywords:
Anaerobic side stream reactor
Complexation
Iron dosing
Sludge reduction mechanisms
Carbon utilization
Wastewater treatment

ABSTRACT

Anaerobic side-stream reactors (ASSRs) can reduce sludge production in activated sludge systems, although the responsible mechanisms remain uncertain. This study evaluated the role of iron dosing in sludge reduction in a sequencing batch reactor (SBR) integrated with an ASSR. A control SBR (SBR.C) and an SBR.M integrated with an ASSR were operated in parallel, with iron concentrations of 1 and 5 mg Fe/L applied sequentially. Increasing iron from 1 to 5 mg Fe/L increased the observed sludge yield from 0.401 to 0.523 g VSS/g COD in SBR.C and from 0.209 to 0.275 g VSS/g COD in SBR.M. However, the relative reduction in observed sludge yield remained approximately 47% at both iron concentrations. The higher iron dose was also associated with lower soluble COD and nutrient concentrations in the ASSR, consistent with greater retention of organic matter and nutrients within the sludge matrix. At 5 mg Fe/L, mass balances showed that direct sludge degradation within the ASSR accounted for only a limited fraction of the lower sludge production. Sludge from SBR.M showed higher substrate uptake and a lower apparent biomass yield, while the additional COD uptake was not accompanied by proportional net polyhydroxyalkanoates or glycogen accumulation. These findings indicate that iron primarily modified organic matter retention within the sludge matrix, whereas the lower sludge production in SBR.M was more associated with altered carbon utilization, in which increased substrate uptake was not accompanied by proportional net biomass formation.

1. Introduction

The abundant sludge production in wastewater treatment plant (WWTP) systems is a significant problem worldwide, accounting for 30–50% of the total operational costs [1]. Currently, sludge treatment is primarily conducted end-of-pipe to reduce sludge volumes. However, several methods for minimizing sludge production in-situ have been reported in the literature, including both chemical and biological approaches [2]. One method is to use an anaerobic side-stream reactor (ASSR) in the return sludge line. The principle of the ASSR is to expose activated sludge to anaerobic redox conditions in an external anaerobic reactor, whereafter it is returned to the main aerobic reactor [3]. Applying an ASSR in the return sludge line can reduce observed sludge yield by 20%-60%, depending on operating conditions [4,5].

Several mechanisms have been proposed to explain this reduction, including direct biomass decay, degradation and subsequent reuse of extracellular polymeric substances (EPS), and altered coupling between substrate utilization and biomass formation under repeated anaerobic–aerobic exposure [6,7]. Operational conditions of ASSR, such as solid retention time (SRT), oxidation-reduction potential (ORP), and sludge interchange ratio (SIR), influence the extent of sludge reduction, indicating that the mechanisms may depend on the intensity and duration of anaerobic exposure [4,8,9]. Recent oxic-settling-anaerobic (OSA)-based configurations have also combined intermittent aeration, attached growth, and side-stream acidogenesis to achieve low net sludge production while maintaining carbon and nutrient removal [10]. Nevertheless, because several biological and physicochemical processes occur simultaneously, their relative contributions to net sludge

* Corresponding author at: Study Program of Environmental Engineering, Department of Biology, Faculty of Science and Technology, Universitas Airlangga, Kampus C UNAIR, Jalan Mulyorejo, Surabaya 60115, Indonesia.
E-mail addresses: M.F.Imron@tudelft.nl, fauzul.imron@fst.unair.ac.id (M.F. Imron).

https://doi.org/10.1016/j.jece.2026.124966
Received 14 July 2026; Received in revised form 21 August 2026; Accepted 4 September 2026
Available online 5 September 2026
2213-3437/© 2026 The Authors. Published by Elsevier Ltd. This is an open access article under the CC BY license (http://creativecommons.org/licenses/by/4.0/).

reduction remain difficult to distinguish.

Iron may further these processes because iron salts are commonly added to wastewater treatment plants for phosphorus removal and can modify sludge transformation through complexation and cation bridging with proteins and humic substances [11,12]. In the Cannibal® system, Fe(III) has been proposed to form complexes with humic substances and protein under aerobic conditions, whereas under anaerobic conditions, reduction of Fe(III) to Fe(II) may destabilize these complexes and release biodegradable substrates that can subsequently be reused during the aerobic phase, thereby contributing to lower sludge production [13,14]. Such reversible interactions between iron and organic matter may also alter substrate accessibility and microbial growth yield under different redox conditions [15]. However, experimental studies on the effect of iron addition in side-stream sludge reduction systems have reported contrasting results. Yagci et al. [15] reported enhanced sludge reduction with increasing iron availability in an OSA system, whereas Semblante et al. [16] observed that iron addition reduced solids destruction and increased retention of organic matter within the sludge matrix. However, our previous physicochemical batch study showed that iron-mediated interactions between proteins and humic substances reduced hydrolysis rates under both aerobic conditions and anaerobic conditions [12]. Furthermore, in our previous long-term reactor experiment, integration of an ASSR with an SBR reduced the observed sludge yield by approximately 42% despite the absence of intentional iron dosing and the presence of only trace iron concentrations [17]. Collectively, these findings show that substantial sludge reduction can occur without deliberate iron addition, while the effect of increasing iron availability on sludge reduction in an ASSR-integrated system remains unresolved.

To address the gap, this study evaluated how iron dosing affects sludge reduction in an SBR integrated with an ASSR. It examined whether increasing iron from 1 to 5 mg Fe/L changed observed sludge yield and organic-matter retention, and whether the lower sludge production in the integrated system was better explained by direct degradation within the ASSR or by changes in carbon allocation under cyclic anaerobic–aerobic conditions. Distinguishing between these mechanisms is practically important because it determines whether ASSR operation should be optimized to enhance direct sludge degradation or to control cyclic redox exposure and biomass growth efficiency. The findings are also relevant to WWTPs that use iron salts for phosphorus removal, because existing iron dosing may affect the sludge reduction benefit expected from ASSR implementation.

2. Materials and methods

2.1. Experimental setup and operational conditions

This experiment used two laboratory-scale treatment systems, as shown in Fig. 1. The first reactor was a 4 L SBR used as a control (SBR.C), and the second reactor was a 4 L SBR (SBR.M) coupled with a 2 L ASSR as the main reactor. All reactors were equipped with stirrers, pH/ORP and DO probes (Endress+Hauser, The Netherlands), peristaltic pumps

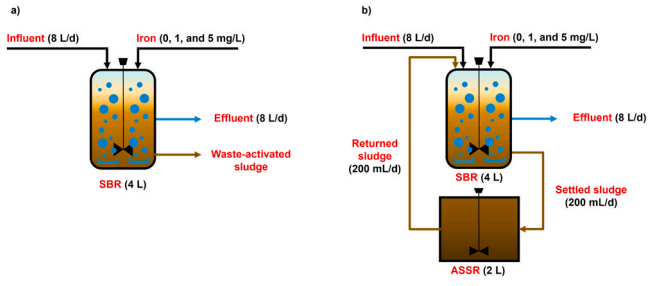


Fig. 1. Two laboratory-scale treatment systems. (a) Control reactor (SBR.C) and (b) main reactor (SBR.M-ASSR).

(Watson-Marlow 120 U/DV-220Du-323, USA), and were automatically controlled by LabVIEW (National Instruments, USA) and a programmable logic controller (National Instruments, USA). The systems operated without temperature control at room temperature (20–22°C).

Both SBRs were inoculated with around 5 g/L of aerobic sludge from Harnaschpolder WWTP in Den Hoorn, the Netherlands. The ASSR was inoculated with 10 g/L of waste-activated sludge originating from the same wastewater treatment plant. Before inoculation, this sludge had been conditioned in a semi-continuous thermophilic sludge-pretreatment reactor operated under anaerobic conditions at 55 °C and an HRT of 5.5 h, as described by Monteiro et al. [18]. Both SBRs were operated on a 4 h per cycle, corresponding to six cycles per day. The cycle included 10 min filling, 50 min anaerobic mixing, 60 min aeration, 45 min anoxic mixing, 60 min settling, 10 min decanting, and 5 min idling. The target DO concentration during aeration was 2–3 mg/L in both SBRs. Each SBR received 8 L/d of synthetic wastewater, corresponding to approximately 1.33 L per cycle and an HRT of 12 h. The SRT of SBR.C was maintained by discharging sludge twice a week. In SBR.M, 200 mL/d of settled sludge was transferred from SBR.M to the ASSR, corresponding to approximately 33 mL per cycle. The transfer was conducted during the idle phase, and the same volume of mixed sludge was returned from the ASSR to SBR.M during the subsequent filling phase. Based on the 2 L ASSR volume and the daily exchange volume, the ASSR SRT was 10 d. The ASSR ORP ranged from −400 to −450 mV. No intentional sludge wasting was applied to SBR.M or the ASSR, apart from routine sampling and solids discharged with the effluent. The calculated SRTs of SBR.C and SBR.M accounted for changes in reactor solids inventory and solids removed through sludge withdrawal, sampling, and effluent discharge. The calculated SRTs during the different operational stages are summarized in Table 1.

The two SBRs were fed with synthetic complex wastewater as described in Gonzalez et al. [19] with an influent COD concentration of 450 ± 64 mg/L. Before the present iron dosing experiment, the same reactor systems had been operated for 175 d with only trace iron concentrations in the influent, following an initial 90 d acclimatization period. The iron dosing experiment was subsequently conducted using the same reactors and biomass without reinoculation. The preceding trace iron period was used only as a historical reference and not as a simultaneous zero iron control. $FeCl_3{\cdot}6\ H_2O$ (Sigma-Aldrich, Germany) was added to the influent to obtain concentrations of 1 and 5 mg Fe/L. These concentrations were selected to represent lower and higher iron concentrations reported for domestic wastewater influent [19,20], allowing the effects of iron concentration to be evaluated. The iron concentrations were applied sequentially to the same reactor systems, beginning with 1 mg Fe/L and followed by 5 mg Fe/L. Each dosing stage was preceded by a 30 d acclimatization period under continuous iron dosing, and data collected during acclimatization were excluded from the analysis. Routine reactor monitoring at 1 mg Fe/L was conducted during cumulative operational days 295–349. During operational days 316–320, corresponding to days 21–25 of the monitored 1 mg Fe/L stage, sodium acetate trihydrate (Merck, Germany) was added to both SBRs during the first minute of the anoxic phase, providing an additional 75 mg COD/L. The addition was discontinued after operational day 320. Routine reactor monitoring at 5 mg Fe/L was conducted during operational days 379–431. Although routine performance monitoring ended on operational day 431, both reactor systems continued to operate without interruption under the same iron-dosing and operational conditions until day 697. Reactor stability during this extended period was followed by monitoring pH, ORP, and DO.

2.2. Batch experiments

2.2.1. Oxygen uptake rate experiment

Endogenous and exogenous oxygen uptake rate (OUR) measurements were conducted to evaluate the respiratory activity of the biomass collected from SBR.C and SBR.M. Sludge samples were collected on

Table 1
Overview of experimental stages and key operational parameters.

Stage	Cumulative operational time (d)	Reactor	HRT	Calculated SRT	OLR (gCOD/L/d)	Iron dose (mg Fe/L)	Use of data
Initial acclimatization	0–90	SBR.C	12 h	n.d.	~0.9	Trace	Excluded
		SBR.M	12 h	n.d.	~0.9	Trace	
		ASSR	10 d	10 d	n.a.	Indirect[1]	
Stage A: trace-iron operation	90–265	SBR.C	12 h	15 d	0.92 ± 0.22	Trace	Historical reference[2]
		SBR.M	12 h	25 d	0.91 ± 0.16	Trace	
		ASSR	10 d	10 d	n.a.	Indirect[1]	
Acclimatization to 1 mg Fe/L	265–295	SBR.C	12 h	n.d.	~0.9	1	Excluded
		SBR.M	12 h	n.d.	~0.9	1	
		ASSR	10 d	10 d	n.a.	Indirect[1]	
Stage B: 1 mg Fe/L	295–349	SBR.C	12 h	16 d	0.90 ± 0.14	1	Included
		SBR.M	12 h	15 d	0.90 ± 0.14	1	
		ASSR	10 d	10 d	n.a.	Indirect[1]	
Acclimatization to 5 mg Fe/L	349–379	SBR.C	12 h	n.d.	~0.9	5	Excluded
		SBR.M	12 h	n.d.	~0.9	5	
		ASSR	10 d	10 d	n.a.	Indirect[1]	
Stage C: 5 mg Fe/L	379–697	SBR.C	12 h	14 d	0.90 ± 0.1	5	Included[3]
		SBR.M	12 h	14 d	0.91 ± 0.14	5	
		ASSR	10 d	10 d	n.a.	Indirect[1]	

Notes:
[1]Iron was dosed to the influent of SBR.M and entered the ASSR indirectly through sludge exchange.
[2]Stage A was used only as a historical reference and not as a simultaneous zero-iron control.
[3]Routine reactor monitoring was conducted during days 379–431, followed by extended operation under the same conditions until day 697.

cumulative operational day 599, during the extended operation at 5 mg Fe/L. The measurements were conducted in triplicate using three separate bottles for each reactor. The experiments were performed in 100 mL nominal-volume Schott bottles (Duran, Germany), which had a total internal capacity of approximately 130 mL. The bottles were completely filled with samples (130 mL) to eliminate headspace. Each bottle was equipped with a DO probe connected to a WTW Multi 3420 (Germany) and stirred at 150 rpm at room temperature. The probe was inserted before the sludge was added, and the bottle was subsequently filled to eliminate the headspace and minimize oxygen transfer from the atmosphere. Before the measurement, sludge samples were aerated until the DO concentration approached saturation. The initial decrease in DO was recorded without external substrate to determine the endogenous OUR. When the DO concentration reached 4 mg/L, 2 mL of sodium acetate stock solution containing 2000 mg COD/L was added to the same bottle without reaeration. The subsequent decrease in DO was recorded to determine the total OUR. The OUR value was calculated from the linear slope of the DO decline during the measurement period. The OUR value is expressed as the volumetric oxygen consumption rate (mg O_2/L/h). The specific oxygen uptake rate (SOUR) is calculated by normalizing the OUR to biomass concentration and thus expressed in mg O_2/gVSS/h. The ΔOUR and ΔSOUR values are then calculated as the difference between the total OUR/SOUR and the endogenous OUR/SOUR, to characterize respiration induced by the external substrate.

2.2.2. Batch yield experiment

A batch yield experiment was conducted to compare the apparent biomass yield and substrate uptake of sludge from SBR.C and SBR.M. Sludge was collected on cumulative operational day 631, while both reactor systems were operated at 5 mg Fe/L. One batch bottle was prepared for each sludge source. Samples collected from each bottle were analyzed in triplicate. The experiments were carried out using a Schott bottle with a working volume of 200 mL. The initial biomass concentration was set at 3.5 gVSS/L. Before use, the sludge was washed three times using a centrifuge (Eppendorf 5910 Ri, Germany) at 8000 rpm for 10 min to remove any remaining substrate residues or dissolved compounds from the bulk liquid. After washing, distilled water was added to the sludge to restore the initial volume. The sludge was then transferred to a Schott bottle, and glucose was added as substrate at an initial concentration of 400 mg COD/L. During the experiment, the bottle was placed on a magnetic stirrer at 150 rpm to maintain suspension homogeneity and was continuously aerated. The batch test was conducted for 24 h, with samples taken at 0, 1, 2, 3, 4, 6, and 24 h. The samples were analyzed for COD and VSS concentrations. The data on changes in COD and VSS were used to calculate the biomass yield, which is the ratio of the increase in VSS to the COD consumed. Additionally, the COD uptake rate was determined by the change in COD concentration over time and then normalized to the biomass concentration.

2.2.3. Intracellular storage polymer experiment

The storage polymer experiment was conducted using fresh sludge collected from SBR.C and SBR.M on cumulative operational day 697, during the extended operation at 5 mg Fe/L. Sludge preparation and experimental conditions were the same as those described for the batch yield experiment in Section 2.2.2, except that an initial working volume of 400 mL was used. The initial biomass concentration was adjusted to 3.5 g VSS/L, and glucose was added to obtain an initial concentration of 400 mg COD/L. The bottles were continuously aerated and stirred at 150 rpm at room temperature throughout the 24 h experiment. Samples were collected at 0, 2, 6, and 24 h for the analysis of intracellular polyhydroxyalkanoates (PHA) and glycogen. Sample preparation and quantification of poly-β-hydroxybutyrate (PHB) and poly-β-hydroxyvalerate (PHV) were performed according to Li et al. [21], whereas sample preparation and glycogen quantification followed the method of Lanham et al. [22]. Net changes in PHA and glycogen were calculated relative to their respective concentrations at 0 h. Total net storage polymer accumulation was calculated as the sum of the net changes in PHA and glycogen and expressed as mg COD/g VSS and mg COD/L.

2.2.4. Biomethane potential (BMP) experiment

The BMP test was conducted to determine the biodegradability of sludge from SBR.C, SBR.M, and ASSR. Sludge samples were collected on cumulative operational day 491, while both SBR systems were operated at 5 mg Fe/L. Each sludge source was analyzed in triplicate using three separate bottles. The experiment was performed using an Automated Methane Potential Test System II (AMPTS II; Bioprocess Control, Sweden). The inoculum for this test was anaerobic sludge taken from Harnaschpolder WWTP in Den Hoorn, the Netherlands, while the substrate was sludge from the three lab reactors. Each measurement was performed in triplicate. A negative control containing only inoculum was analyzed, as well as a positive control containing inoculum and cellu-

lose. The inoculum-to-substrate ratio is 2:1, with a total mixture volume of 400 mL in a 500 mL Schott bottle (Duran, Germany). The recipes and dosages of macronutrients, micronutrients, and phosphate buffer were based on Angelidaki et al. [23]. BMP ultimate was determined based on Eq. (1).

$$BMP_t = B_0(1 - e^{-k \bullet t}) \quad (1)$$

BMPt is the cumulative methane production at time *t* (NmL CH_4/gVS), B_0 is the ultimate methane potential (BMP ultimate), *k* is the methane production rate constant (/d), *t* is the digestion time (d). By plotting *t* as the x-axis and *BMPt* as the y-axis, the BMP ultimate was determined based on the nonlinear curve fitting. Curve fitting was conducted using MATLAB R2023b (MathWorks, USA).

2.3. Analytical methods

2.3.1. Sludge yield calculation

Mixed liquor volatile suspended solids (MLVSS) are used to calculate sludge production. Observed sludge yield (Y_{obs}) is calculated based on the slope of the linear regression of the plot between cumulative consumed substrate (g COD; x-axis) and cumulative sludge production (g VSS; y-axis) (Eq. 2). Sludge reduction is calculated based on Eq. (3).

$$Y_{obs} = \frac{X}{S} = \frac{\Delta X_{SBR} V_{SBR} + \Delta X_{ASSR} V_{ASSR} + \sum (X_{SBR} Q_{SBR.waste} + X_{ASSR} Q_{ASSR.waste} + X_{Eff} Q_{Eff}) \Delta t}{\sum (S_{in} Q_{in} - S_{Eff} Q_{Eff}) \Delta t} \quad (2)$$

$$Sludge\ reduction\ (\%) = \frac{Y_{obs}SBR.C - Y_{obs}SBR.M}{Y_{obs}SBR.C} \times 100\% \quad (3)$$

In Eq. (2), ΔX_{SBR}, ΔX_{ASSR}, and Δt are the change in sludge (g VSS/L) in SBR and ASSR, and time (d), respectively. V_{SBR} and V_{ASSR} are the volumes of SBR and ASSR (L), respectively. $Q_{SBR\ waste}$, Q_{in}, and Q_{eff} are the flow rates of waste sludge from SBR, influent, and effluent (L/d), respectively. $Q_{ASSR\ waste}$ is the flow rate of sludge from ASSR generated during sampling for analysis. S_{in} and S_{eff} are the substrate concentrations of influent and effluent (g COD/L), respectively.

2.3.2. Parameters

Mixed liquor suspended solids (MLSS) and MLVSS in SBR and ASSR, both in influent, effluent, and discharged sludge, were analyzed based on Standard Methods [24]. Total chemical oxygen demand (COD), soluble COD (sCOD), NH_4^+-N, NO_2^--N, NO_3^--N, and PO_4^{3-}-P/Total phosphate (TP) were measured using spectrophotometric test kits (Hach Lange LCK, Germany). The respective kit codes are as follows: LCK 114, LCK 314, LCK 303, LCK 341, LCK 339, LCK 348. The sample was first filtered using a 10 mL syringe equipped with a 0.45 µm CHROMAFIL Xtra PES-45/25 filter (Macherey-Nagel, Germany) for all parameters, then analyzed with the Hach kit, except for total COD and TP.

To assess intracellular energy status and oxidative stress responses, the ATP content of sludge samples from SBR.C, SBR.M, and ASSR was measured using the Bugcount Solids Test Kit (Biotechnology Solutions (BTS), USA) and quantified with a luminometer (LuminUltra PhotonMaster Luminometer, Canada). Superoxide dismutase (SOD) activity was measured using a colorimetric assay kit (Thermo Fisher Scientific, USA) according to the manufacturer's instructions. For SOD activity, sludge was extracted in phosphate-buffered saline (PBS) and centrifuged prior to analysis. The assay was performed in 96-well microplates, and absorbance was measured at 450 nm using a FLUOstar Galaxy Multifunctional Microplate Reader (BMG Technologies, UK). SOD activity was normalized to the protein content and expressed as U/mg protein.

Soluble EPS (S-EPS) was extracted by centrifuging sludge at 8000 rpm for 10 min, followed by filtering the supernatant through a 10 mL syringe fitted with a 0.45 µm filter. The pellet was resuspended in 0.5% NaCl and then vortexed to obtain loosely bound EPS (LB-EPS) from the same sludge. Subsequently, the mixed pellet was centrifuged at 8000 rpm for 10 min, and the supernatant was filtered using a 10 mL syringe equipped with a 0.45 µm filter to obtain LB-EPS. Tightly bound EPS (TB-EPS) from the same sample was resuspended in 0.5% NaCl, vortex-mixed, and then heated in a water bath at 60°C for 1 h. The sample was then centrifuged at 8000 rpm for 10 min, after which the supernatant was filtered using a 10 mL syringe equipped with a 0.45 µm filter to obtain TB-EPS. The EPS concentration was calculated from the carbohydrate and protein concentrations, measured via the sulfuric acid method [25] and the modified Lowry method [26], respectively.

To determine the concentration of soluble Fe(III)/Fe(II) in sludge, the sludge was centrifuged at 8000 rpm for 10 min, and the supernatant was filtered using a 10 mL syringe equipped with a 0.45 µm filter to obtain soluble iron and then measured using spectrophotometric test kits (Hach Lange LCK, Germany; kit code LCK 312). To determine the total iron concentration in the sludge, the sludge is digested in a microwave digester for 30 min with nitric acid. Then, the digested sludge is filtered through a 10 mL syringe fitted with a 0.45 µm filter to obtain soluble iron. Subsequently, total Fe was measured by ICP-OES (Agilent 5800, USA).

With iron dosing, there is also the potential for crystal phase formation in sludge. For crystal phase analysis, sludge from SBR and ASSR before and after iron dosing was freeze-dried under dark conditions to prevent oxidation of ferrous iron. XRD assessment was used to identify the crystal phase in sludge using a Bruker Discover D8 (Bruker, USA) with Cu-Kα radiation. The diffraction pattern was recorded at 2θ with a range of 5–120° in steps of 0.02°.

2.3.3. Mass balance calculations

COD, nitrogen, and VSS mass balances were constructed from one sampling campaign conducted during operation at 5 mg Fe/L. Daily loads were obtained by multiplying the measured concentrations by the corresponding flow rates. Separate unit balances were established for SBR.C, SBR.M, and the ASSR. For SBR.C, the influent was considered the input, while the effluent and wasted sludge were considered the outputs. For SBR.M, the external influent and sludge returned from the ASSR were considered inputs, while the effluent and sludge transferred to the ASSR were considered outputs. The latter two sludge streams formed the input and output of the ASSR balance, respectively.

COD loads were determined from directly measured total COD concentrations. Estimated COD removal in each SBR was calculated as the difference between the total incoming and outgoing loads. For the ASSR, the difference between incoming and outgoing COD loads was reported as the net COD decrease.

For the nitrogen balance, organic nitrogen was calculated using Eq. (4):

$$N_{organic} = TN - NH_4^+\text{-N} - NO_2^-\text{-N} - NO_3^-\text{-N} \quad (4)$$

where $N_{organic}$ is the organic nitrogen concentration, *TN* is the total nitrogen concentration, and NH_4^+-*N*, NO_2^--*N*, and NO_3^--*N* are the measured total and inorganic nitrogen concentrations. Nitrogen conversion in each SBR was determined from the difference between the

total incoming and outgoing nitrogen loads. Organic-N reduction and NH_4^+-N release across the ASSR were determined from their respective load differences.

The net VSS decrease across the ASSR was calculated using Eq. (5):

$$\Delta M_{VSS,ASSR} = Q_{in}X_{VSS,in} - Q_{out}X_{VSS,out} \quad (5)$$

where $\Delta M_{VSS,ASSR}$ is the net VSS decrease (g VSS/d), Q_{in} and Q_{out} are the sludge flow rates entering and leaving the ASSR (L/d), $X_{VSS,in}$ and $X_{VSS,out}$ are the corresponding MLVSS concentrations (g VSS/L). Both flow rates were 0.2 L/d. No COD-to-VSS conversion was applied. For comparison with the organic-N balance, the net VSS decrease was converted to a biomass-associated nitrogen equivalent using 0.06 g N/g VSS [27,28]. The apparent ASSR contribution to the overall sludge-production difference was calculated by dividing its net VSS decrease by the difference in daily sludge production between SBR.C and the integrated system. Because the balances were based on one sampling campaign, the results were treated as descriptive estimates.

2.3.4. Microbial community analysis

Sludge samples were collected from SBR.C, SBR.M, and the ASSR on cumulative operational day 470, during operation at 5 mg Fe/L. Samples from SBR.C and SBR.M were collected after the aerobic phase, while ASSR samples were collected at the corresponding sampling time. Three sludge subsamples were collected from each reactor. These represented within-reactor sampling replicates rather than independently operated reactor replicates. DNA was extracted using the FastDNA® SPIN Kit for Soil (MP Biomedicals, USA), and DNA concentrations were assessed using a Qubit 3.0 fluorometer and the Qubit® dsDNA HS Assay Kit.

The V3–V4 region of the bacterial 16S rRNA gene was amplified using primers 341 F (5′-CCTAYGGGRBGCASCAG-3′) and 806 R (5′-GGACTACNNGGGTATCTAAT-3′). Amplicons were sequenced on an Illumina platform using 2 × 250 bp paired-end sequencing by Novogene Co., Ltd. Sequence processing was performed using QIIME2 version 202202. After read merging, quality filtering, and chimera removal, amplicon sequence variants (ASVs) were generated using the DADA2 denoising workflow. Taxonomic assignment was performed using the QIIME2 classify-sklearn algorithm with a classifier trained against the SILVA 138.1 database.

Functional potential was predicted separately from the taxonomic classification using PICRUSt2 version 2.3.0. ASV representative sequences and their corresponding feature abundance table were used for functional inference. Predicted gene-family abundances were annotated using the Kyoto Encyclopedia of Genes and Genomes (KEGG) Orthology database. Prediction quality was evaluated using abundance-weighted nearest-sequenced taxon index values, which ranged from 0.339 to 0.481 across the nine samples. Because PICRUSt2 infers functions from marker-gene profiles, the resulting KEGG ortholog abundances were interpreted as predicted functional potential rather than directly measured gene expression or metabolic activity.

2.3.5. Statistical analysis

The experiment comprised one SBR.C and one coupled SBR.M–ASSR system, with iron concentrations of 1 and 5 mg Fe/L applied sequentially to the same reactors. Consequently, the reactor configurations and iron dosing stages were not independently replicated. Each routine reactor monitoring point represented a single analytical determination from one sampling event and is presented as such in applicable figures. Routine monitoring data, including COD, nutrients, SVI, and soluble compounds in the ASSR, are reported as the mean ± standard deviation of the observations collected during each operational stage. For EPS, ATP, SOD activity, and iron measurements, results are presented as the mean ± standard deviation of three separately collected sludge samples. OUR/SOUR and BMP results are presented as the mean ± standard deviation of three parallel batch bottles. Where applicable, differences among reactor-derived sample groups and iron-dosing stages were evaluated using one-way analysis of variance (ANOVA) in IBM SPSS Statistics version 29.0.2.0 (IBM Corp, USA), with statistical significance defined at $p < 0.05$. For the batch yield experiment, one batch bottle was used for each sludge source, and analytical measurements were performed in triplicate. The reported variation therefore represents analytical variability rather than independent experimental replication. Storage polymer measurements were performed as single determinations and are presented without error bars. Uncertainty in the observed sludge yield was reported as the standard error of the regression slope. Microbial-community triplicates represented separate sludge subsamples from the same reactor rather than independently operated reactor replicates; therefore, no inferential statistical analysis was used to establish differences among reactor configurations.

3. Results and discussion

3.1. Reactor performance during iron dosing

COD removal remained relatively stable at approximately 80–90% in both SBR.C and SBR.M during operation at 1 and 5 mg Fe/L, with effluent COD concentrations generally below 100 mg/L (Figs. 2a and 2b). At each iron dose, the COD removal performance of SBR.M was comparable to that of SBR.C, indicating that ASSR circulation did not deteriorate COD removal. The effects of ASSR integration on nitrogen conversion were less uniform. At both iron doses, SBR.C maintained NH_4^+-N removal above 90%, whereas SBR.M showed lower and more variable ammonium removal (Figs. 2c and 2d). On a mass load basis, NH_4^+-N removal was approximately 321 and 243 mg N/d for SBR.C and SBR.M, respectively, at 1 mg Fe/L, and 464 and 427 mg N/d at 5 mg Fe/L. The net NH_4^+-N load returned from the ASSR was small, accounting for only about 2.2% and 0.9% of the external influent load at 1 and 5 mg Fe/L, respectively, and therefore could not explain the lower conversion in SBR.M. The lower and fluctuating DO in SBR.M (approximately 0.3–2.0 mg/L) and repeated anaerobic exposure of the recycled sludge may have contributed, although their individual effects could not be distinguished. In addition, denitrification was incomplete, resulting in NO_3^--N in the effluent of both reactors (5–30 mg/L). No consistent difference was observed between SBR.C and SBR.M under the same iron dosing conditions. The addition of sodium acetate during days 21–25 of the 1 mg Fe/L stage resulted in a marked decrease in effluent NO_3^--N in both reactors, indicating that nitrate reduction was limited by the availability of readily biodegradable COD during the anoxic phase. TP removal remained within approximately 20–50% in both reactors at both iron doses and showed no clear dose-dependent improvement (Figs. 2e and 2f). The influent Fe:P molar ratios were approximately 0.06:1 at 1 mg Fe/L and 0.30:1 at 5 mg Fe/L, both below the theoretical minimum ratio of approximately 1:1 commonly associated with stoichiometric iron–phosphate binding. Competition for readily biodegradable COD between denitrifying organisms and phosphate-accumulating organisms (PAO), due to nitrate transfer to the anaerobic phase, may also have constrained biological phosphorus removal, while fluctuating aeration in SBR.M may have further affected process stability [29–31].

3.2. Effects of iron dosing on sludge yield and characteristics

The observed sludge yield of SBR.C and SBR.M is shown in Fig. 3 for iron dosing at 1 and 5 mg Fe/L. Based on Fig. 3, increasing iron dosage from 1 to 5 mg Fe/L increased the observed sludge yield in both configurations. In SBR.C, the observed sludge yield increased from 0.401 ± 0.007 to 0.523 ± 0.014 g VSS/g COD, while in SBR.M, the observed sludge yield also increased from 0.209 ± 0.006 to 0.275 ± 0.009 g VSS/g COD. This suggests that the higher observed sludge yield was partly linked to Fe(III)-mediated retention of organic matter, likely through cation bridging and complexation within the sludge matrix [32]. The findings of this study were aligned with Semblante et al. [16], which

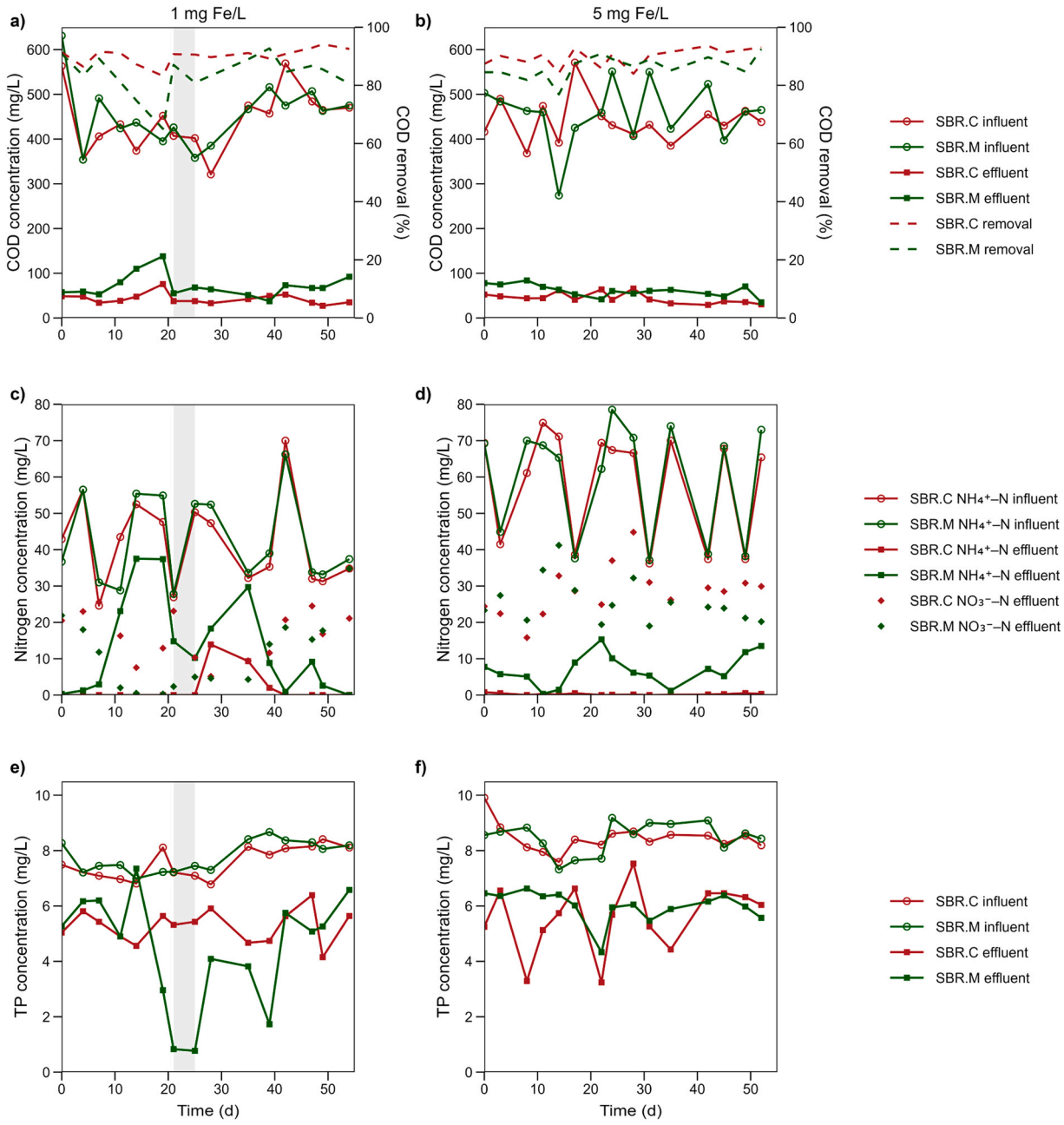


Fig. 2. Performance of SBR.C and SBR.M at 1 mg Fe/L and 5 mg Fe/L. (a,b) COD concentration and removal, (c,d) NH_4^+-N and NO_3^--N concentrations, and (e,f) TP concentration. Panels (a), (c), and (e) show data at 1 mg Fe/L, while panels (b), (d), and (f) show data at 5 mg Fe/L. The shaded area in panels (a), (c), and (e) indicates days 21–25, during which an external soluble COD source was temporarily added to both reactors.

demonstrated that increasing iron concentration in an SBR integrated with an OSA system also increased observed sludge yield when compared to an SBR without iron addition. Although the observed sludge yield increased, the contribution of the ASSR in lowering the net sludge yield/ sludge reduction remained unchanged (~47%) for both iron dosing levels, while our previous study reported approximately 42% sludge reduction in the integrated SBR.M–ASSR system operated without iron addition [17]. These findings suggest that iron dosing influences sludge physicochemical properties and contributes to the increase in observed sludge yield, but is unlikely to be the primary factor governing the lower sludge production in the integrated system.

Further investigation of this behavior showed that increasing the iron dosage from 1 to 5 mg Fe/L decreased the concentrations of sCOD, NH_4^+-N, and PO_4^{3-}-P in the ASSR, as shown in Fig. 4. sCOD decreased from an average of 105 ± 54 mg/L to 47.3 ± 10.4 mg/L. NH_4^+-N decreased from 50.4 ± 11.3 mg/L to 29 ± 4.8 mg/L and PO_4^{3-}-P decreased from 91.2 ± 17.8 mg/L to 41.3 ± 8.1 mg/L. These differences were unlikely to result solely from changes in solids transfer to the ASSR. The SVI of SBR.M remained similarly high at both iron doses, ranging from approximately 206–250 mL/g. Although sludge compaction was poor, a settled sludge layer remained recoverable after the 60 min settling phase. The fixed exchange volume of 200 mL/d was withdrawn from the lowest part of this settled layer, corresponding to approximately 33 mL per cycle. This entails that the best settling sludge was transferred to the ASSR, which could have enhanced the high SVI of the remaining sludge. The MLVSS concentration of the transferred sludge remained broadly comparable at 1 and 5 mg Fe/L, averaging 6466 ± 1072 and 5973 ± 631 mg/L, respectively (Figure S1). Thus, the lower soluble

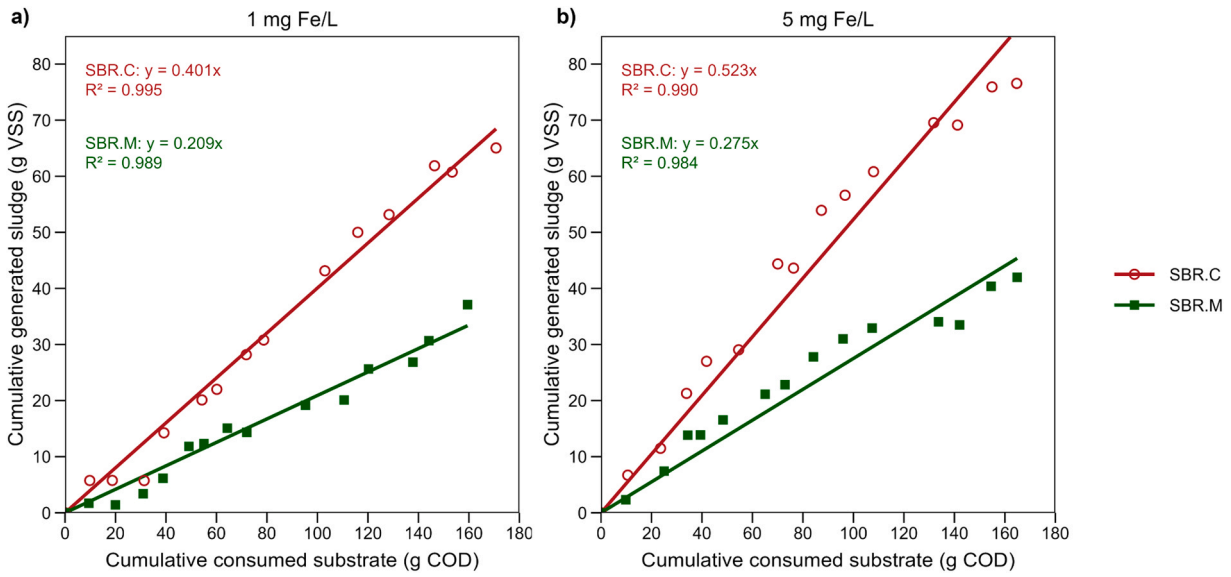


Fig. 3. Relationship between cumulative consumed substrate and cumulative generated sludge for determining the observed sludge yield in (a) 1 mg Fe/L and (b) 5 mg Fe/L.

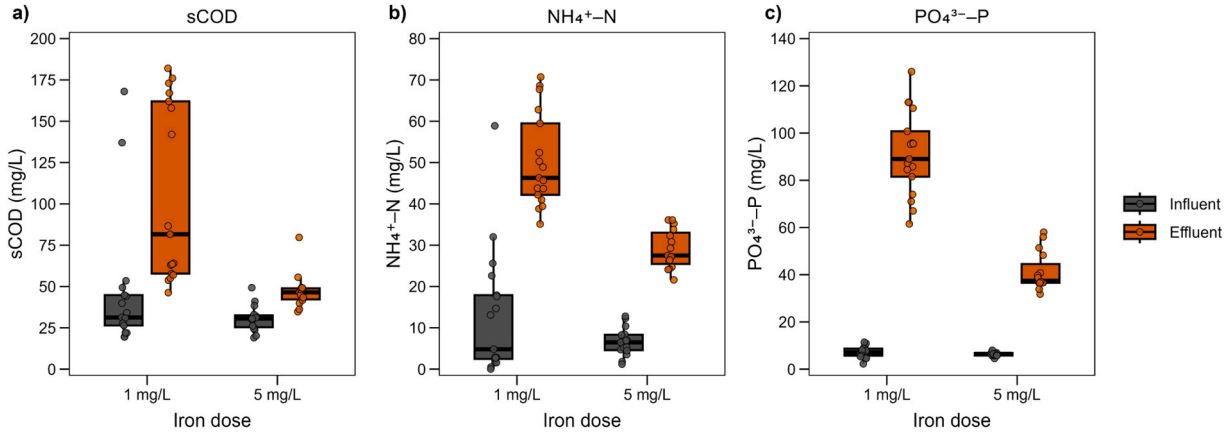


Fig. 4. Boxplots of (a) sCOD, (b) NH_4^+-N, and (c) PO_4^{3-}-P concentrations in the influent and effluent of the ASSR at 1 and 5 mg Fe/L.

concentrations of COD, NH_4^+-N, and PO_4^{3-}-P at 5 mg Fe/L were not associated with improved settling or a substantial change in the solids concentration entering the ASSR. Instead, the results are consistent with greater retention of organic matter and nutrients within the sludge matrix at the higher iron dose, thereby limiting their release into the liquid phase under anaerobic conditions [16].

Despite the consistently high SVI, no uncontrolled sludge washout occurred. Effluent TSS concentrations were 84 ± 50 and 111 ± 63 mg/L in SBR.C and SBR.M, respectively, at 1 mg Fe/L, and 114 ± 63 and 128 ± 70 mg/L at 5 mg Fe/L. SBR.M showed somewhat higher effluent solids concentrations, but the difference was limited relative to the overall difference in sludge production. Moreover, the effluent VSS load was included in the cumulative sludge production calculation. Consequently, the lower observed sludge yield in SBR.M cannot be attributed to unaccounted solids washout. Nevertheless, the high SVI demonstrates that poor settleability remained an important operational limitation of the integrated SBR–ASSR system that might be tackled by a different sludge selection prior to recycling to the ASSR.

To understand the higher stability of the sludge with increased iron dosing, the EPS distribution was examined and is shown in Fig. 5. Increasing the iron concentration led to a significant increase in TB-EPS from 33.87 ± 1.55 to 42.66 ± 0.39 mg/gVSS in SBR.C ($p < 0.05$), whereas only a slight increase was observed in SBR.M from 41 ± 0.8 to 42.37 ± 1.9 mg/gVSS. At the same time, LB-EPS increased significantly in SBR.M from 0.81 ± 0.04 to 4.07 ± 1.95 mg/gVSS and in SBR.C from 0.5 ± 0.1 to 3.09 ± 0.34 mg/gVSS ($p < 0.05$), while S-EPS showed a slight increase in both SBR.C and SBR.M but a decrease in ASSR ($p > 0.05$). The distribution of iron between the sludge and liquid phases was further examined under 5 mg Fe/L iron dosing conditions and is presented in Figs. 5b and 5c. The sludge-associated iron content was highest in SBR.C, reaching 34.6 ± 0.4 mg/g dry sludge, followed by SBR.M at 31.4 ± 0.4 mg/g dry sludge and ASSR at 24.6 ± 0.3 mg/g dry sludge. This indicates that iron was retained in the sludge matrix of all reactors, particularly in the SBRs. In contrast, the ASSR showed lower sludge-associated iron than the SBRs, while soluble iron concentrations were substantially higher. Total soluble iron remained relatively low in the SBRs, with a range of 0.1 – 0.5 mg/L, whereas the ASSR contained 2.3 mg/L of soluble iron. This suggests that part of the iron associated with the sludge from SBR.M was redistributed into the liquid phase under anaerobic conditions. Nevertheless, the remaining sludge-associated iron in the ASSR may still have contributed to EPS binding and structural reorganization, as indicated by the increase in TB-EPS and the absence of an increase in S-EPS. Since Fe(III) remained dominant over Fe(II) in the ASSR, the increase in soluble iron was not governed

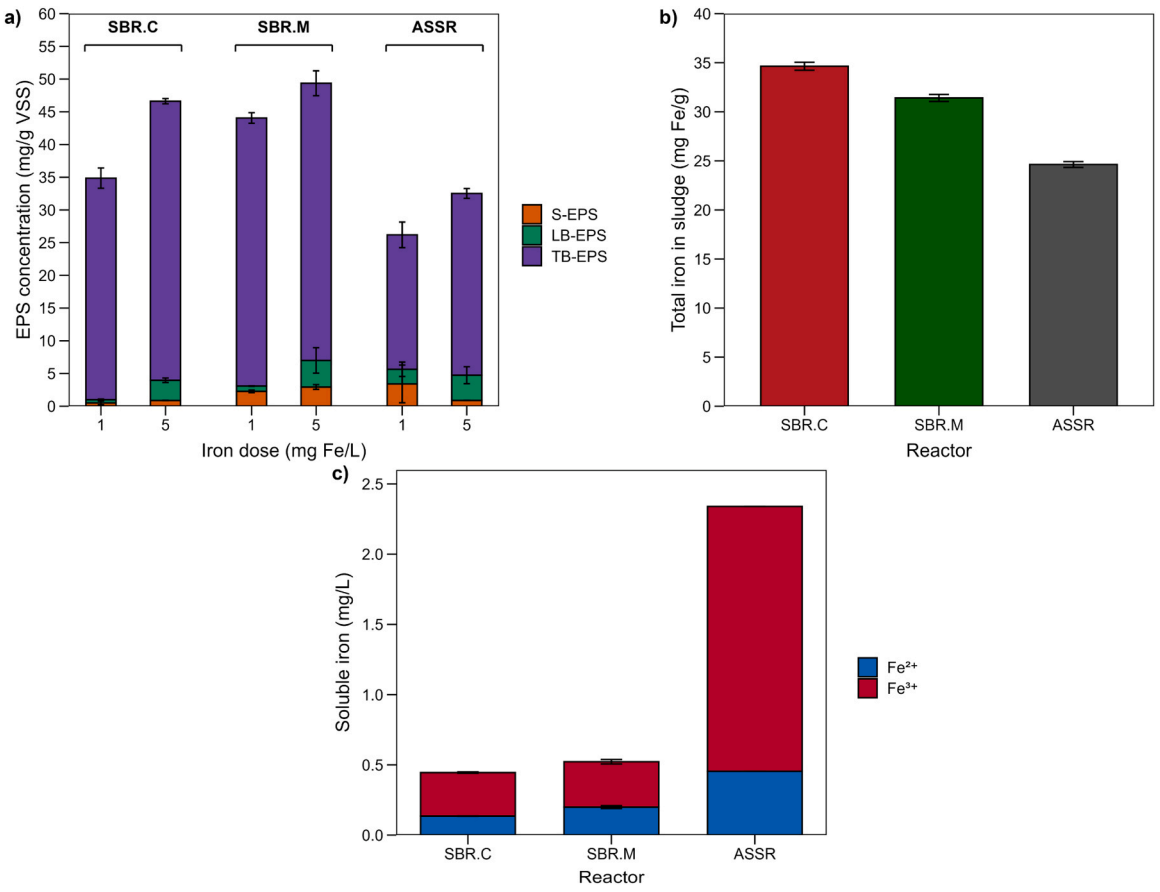


Fig. 5. (a) S-EPS, LB-EPS, and TB-EPS concentrations at 1 and 5 mg Fe/L, (b) total iron concentration in sludge, and (c) soluble iron concentrations at 5 mg Fe/L in SBR.C, SBR.M, and ASSR.

solely by the reduction of Fe(III) to Fe(II), but may also involve iron complexation with soluble organic compounds or the release of iron-associated compounds from the sludge matrix.

A similar observation was reported by Semblante et al. [16], who found that increasing iron dosing to 15 mg Fe/L in an SBR-OSA system also increased TB-EPS accumulation. The increase in TB-EPS suggests the formation of more compact and stable EPS matrices, likely driven by iron-induced cross-linking between EPS components such as proteins and humic substances [12,33]. Multivalent cations such as Fe(III) can act as bridging agents, strengthening intermolecular interactions and promoting the aggregation of organic matter into tightly bound fractions [33,34]. The XRD results shown in Figure S2 indicated changes in sludge crystallinity following iron addition. Without iron dosing, the XRD pattern was dominated by amorphous phases with some crystal peaks typical of activated sludge. The presence of 5 mg Fe/L iron led to the appearance of additional crystalline phases, with the amorphous component still predominant. These crystalline phases were also present in the ASSR, suggesting their stability in anaerobic conditions.

3.3. COD, nitrogen, and VSS mass balances

The COD balance (Fig. 6) showed that SBR.M received a higher total COD load than SBR.C because its calculation included the sludge returned from the ASSR. Based on the measured effluent and sludge output loads, the COD mass balance recovery was 41% in SBR.C and 44% in SBR.M. The remaining balance differences, reported as estimated removed COD, were 2097 mg COD/d in SBR.C and 2988 mg COD/d in SBR.M, corresponding to 59% and 56% of their respective total COD inputs. Although the absolute estimated removed COD was higher in SBR.M, this system produced less sludge than SBR.C, suggesting that a

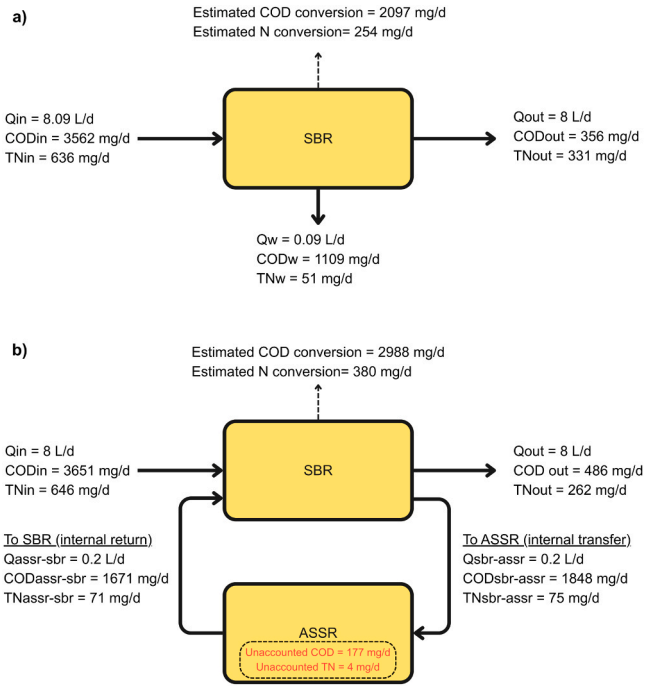


Fig. 6. Mass balance of COD and nitrogen in (a) SBR.C and (b) SBR.M with 5 mg Fe/L iron addition.

smaller fraction of the transformed COD was incorporated into net biomass. Previous studies have proposed that, under cyclic anaerobic–aerobic conditions, part of the substrate may be directed towards non-growth-associated processes [35,36]. However, the contribution of such processes could not be quantified from the present mass balance.

For nitrogen, the measured mass balance recovery in the effluent and sludge output streams was 60% in SBR.C and 47% in SBR.M. The remaining balance differences, reported as estimated nitrogen conversion, were 254 mg N/d in SBR.C and 380 mg N/d in SBR.M, corresponding to 40% and 53% of their respective TN inputs (Fig. 6 and Table S1). Across the ASSR, 71 of the 75 mg N/d entering through the transferred sludge was recovered in the sludge returned to SBR.M, corresponding to a measured TN mass balance recovery of 95%. At the component level, the organic-N load decreased by approximately 6.5 mg N/d, while the NH_4^+-N load increased by 4.5 mg N/d. The directly measured VSS decrease across the ASSR was approximately 0.11 g VSS/d, corresponding to 6.6 mg sludge-associated N/d based on the assumed N/VSS ratio. The close agreement between the organic-N decrease and the nitrogen equivalent derived from the VSS decrease supports the occurrence of direct solids degradation within the ASSR, although its extent was limited under the tested conditions.

Daily sludge production was 1.48 g VSS/d in SBR.C and 0.80 g VSS/d in SBR.M, corresponding to an overall difference of 0.68 g VSS/d. This direct VSS loss within the ASSR accounted for 16.2% of the difference, compared with approximately 25% during operation without intentional iron dosing. However, because the two mass balance assessments were conducted during different operational periods and no corresponding balance was available at 1 mg Fe/L, the difference between these estimates cannot be attributed specifically to iron dosing. Moreover, the limited organic-N decrease and NH_4^+-N release do not support extensive anaerobic destabilization and hydrolysis of iron-associated proteins as the dominant sludge-reduction pathway at 5 mg Fe/L, as proposed by Novak et al. [13] and Park et al. [14]. Overall, the results indicate that most of the lower sludge production originated from reduced net solids production in SBR.M rather than direct sludge degradation in the ASSR, although the underlying carbon allocation pathways could not be resolved from the mass balance alone.

3.4. Carbon utilization and physiological responses

Fig. 7 shows distinct substrate utilization patterns between sludge from SBR.C and SBR.M. In the glucose fed batch experiment, SBR.M exhibited a lower apparent biomass yield than SBR.C, at 0.26–0.34 and 0.55–0.72 g VSS/g COD, respectively (Fig. 7a). In contrast, the maximum COD uptake rate was higher in SBR.M, reaching 20.5 ± 0.02 mg COD/g VSS/h compared with 9.7 ± 0.06 mg COD/g VSS/h in SBR.C (Fig. 7b). After reaching this peak, the COD uptake rate in SBR.M declined and remained at lower levels until 24 h. Thus, the faster initial substrate uptake in SBR.M was not translated into proportional biomass formation, indicating weaker coupling between substrate utilization and growth [37].

Storage polymer analysis was used to assess whether part of the COD that was not converted into biomass was temporarily retained as PHA or glycogen (Fig. 7c). During the first 6 h, net storage polymer accumulation relative to the initial content reached 21.8 mg COD/g VSS (76 mg COD/L) in SBR.C, mainly due to an increase in PHA of 14.3 mg COD/g VSS (49.7 mg COD/L). In comparison, SBR.M showed a higher net storage accumulation of 26.3 mg COD/g VSS (99.8 mg COD/L), predominantly due to glycogen accumulation of 20.6 mg COD/g VSS (78.4 mg COD/L). After 24 h, net storage accumulation in SBR.C remained relatively stable at 20.7 mg COD/g VSS (72.1 mg COD/L), with PHA accounting for 19.4 mg COD/g VSS (67.6 mg COD/L). Conversely, the storage products in SBR.M decreased to 14.2 mg COD/g VSS (54 mg COD/L), consisting mainly of glycogen at 13.7 mg COD/g VSS (52.1 mg

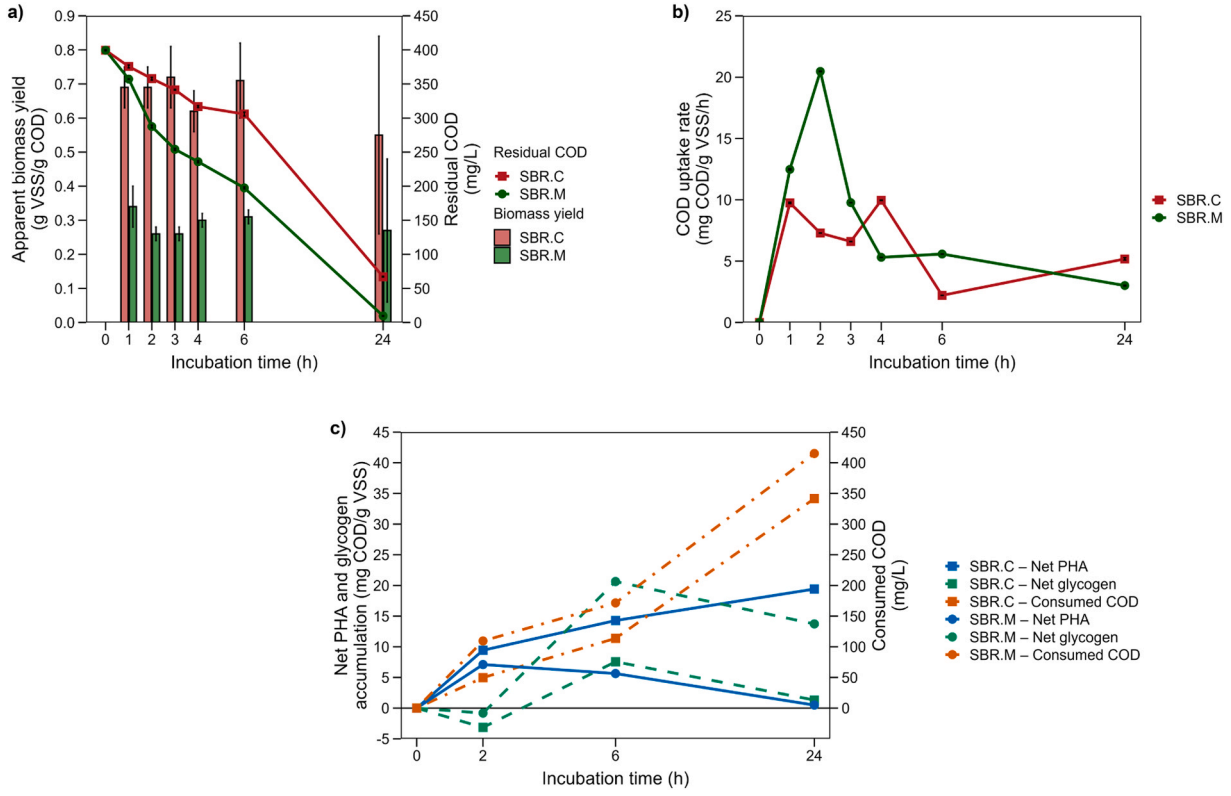


Fig. 7. Carbon utilization during batch experiments with sludge from SBR.C and SBR.M. (a) apparent biomass yield and residual COD, (b) COD uptake rate, and (c) net PHA and glycogen accumulation and consumed COD.

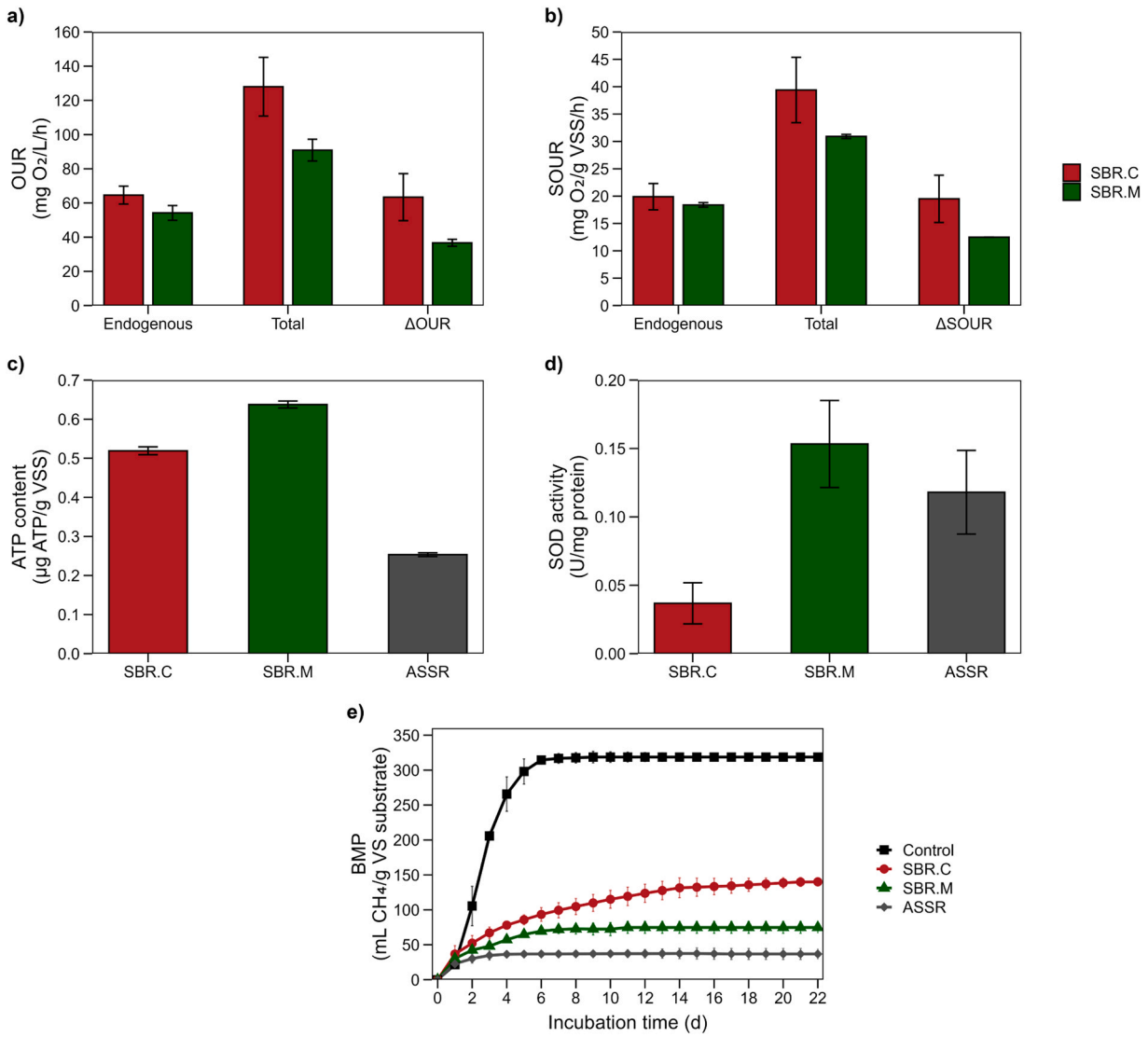


Fig. 8. Bioenergetic and physiological characteristics of sludge from SBR.C, SBR.M, and ASSR during operation at 5 mg Fe/L. (a) OUR, (b) SOUR, (c) ATP content, (d) SOD activity, and (e) BMP.

COD/L), while net PHA accumulation was only 0.5 mg COD/g VSS (1.9 mg COD/L). This occurred despite the higher cumulative COD consumption in SBR.M than in SBR.C, at 415 and 341 mg COD/L, respectively. Intracellular storage allows rapidly assimilable substrate to be retained during substrate-rich periods and subsequently mobilized when external substrate availability decreases [38,39]. Therefore, the results indicate that SBR.M initially directed more carbon toward glycogen storage but subsequently mobilized a substantial part of the stored carbon. Consequently, its lower biomass yield cannot be explained by greater persistent storage polymer accumulation, but rather reflects a different distribution and subsequent utilization of the consumed carbon.

The bioenergetic and physiological measurements were consistent with this altered carbon utilization pattern (Fig. 8). The substrate-induced ΔOUR and ΔSOUR were lower in SBR.M, at 36.7 ± 2 mg O_2/L/h and 12.5 ± 0.03 mg O_2/g VSS/h, respectively, than in SBR.C, at 63.4 ± 13.7 mg O_2/L/h and 19.5 ± 4.3 mg O_2/g VSS/h (Fig. 8a–b). This indicates a weaker aerobic respiratory response to substrate addition in SBR.M. Combined with its faster COD uptake and lower apparent biomass yield, the results suggest that the consumed substrate was not proportionally directed toward either immediate aerobic oxidation or biomass synthesis. Meanwhile, ATP content (Fig. 8c) remained slightly higher in SBR.M than in SBR.C, at 0.637 ± 0.01 and 0.519 ± 0.01 μg ATP/g VSS, respectively, indicating that the lower growth efficiency was not associated with depletion of the intracellular ATP pool.

Previous studies have attributed sludge reduction in ASSR systems to metabolic uncoupling, in which catabolic energy generation becomes less efficiently coupled to biomass synthesis [36,40]. However, the combination of maintained ATP content and lower substrate-induced respiration in SBR.M does not correspond to a simple ATP-deficient uncoupling mechanism. Instead, the substantially lower ATP content in the ASSR sludge, at 0.253 ± 0.005 μg ATP/g VSS, is consistent with the consumption of intracellular energy reserves during anaerobic exposure. The lower ATP content in the ASSR than in SBR.M is consistent with greater use of intracellular energy reserves during anaerobic exposure and possible replenishment under aerobic conditions. This suggests that part of the substrate-derived energy may have been allocated to ATP recovery rather than biomass synthesis [41,42]. Because ATP content reflects the intracellular energy pool rather than its production and turnover rates, this interpretation does not quantify the associated energy demand.

SOD activity was higher in SBR.M than in SBR.C, at 0.15 ± 0.03 and 0.04 ± 0.02 U/mg protein, respectively (Fig. 8d). This indicates a stronger cellular stress response, which may be associated with repeated

transitions between anaerobic and aerobic conditions and the resulting formation of reactive oxygen species [43]. Energy requirements for redox regulation, cellular protection, and recovery may consequently contribute to non-growth-associated substrate utilization. Nevertheless, SOD activity and ATP content do not directly quantify maintenance energy. Therefore, increased maintenance demand should be considered a plausible contributing process rather than a demonstrated mechanism.

The BMP results further showed that sludge from SBR.M and the ASSR had a lower biomethane potential, at 75 ± 9 and 38 ± 6 mL CH_4/g VS, respectively, than sludge from SBR.C, at 140 ± 11 mL CH_4/g VS (Fig. 8e and Table S2). These results indicate that less anaerobically biodegradable organic matter remained in sludge from the integrated system, although they do not identify the preceding carbon transformation pathway. Overall, the results support altered carbon utilization and physiological adaptation in SBR.M, characterized by faster substrate uptake, different storage polymer turnover, lower substrate-induced respiration, and lower biomass formation. This behavior does not provide conclusive evidence of classical metabolic uncoupling, while increased non-growth-associated energy demand remains a possible contributor to the reduced growth efficiency.

3.5. Microbial community and predicted functional potential

The microbial community composition differed among SBR.C, SBR.M, and the ASSR, providing supporting evidence for their contrasting physiological characteristics, as shown in Fig. 9. At the family level (Fig. 9a), SBR.C was dominated by Rhodocyclaceae (13.49%) and Haliangiaceae (15.32%), which are commonly associated with active heterotrophic growth and substrate assimilation in conventional activated sludge systems [44,45], consistent with the higher biomass yield observed in SBR.C. In contrast, SBR.M showed a clear shift toward groups such as Gemmatimonadaceae (11.78%), which are often linked to oligotrophic conditions [46], and several hydrolytic groups, such as Saprospiraceae (5.14%) and Fibrobacteraceae (6.19%), are involved in the degradation of complex organic substrates [47,48]. The ASSR community further reinforces this pattern, with enrichment of Chitinophagaceae (13.74%), Saprospiraceae (8.26%), and Bacteroidetes vadinHA17 (6.29%), indicating a strong potential for hydrolysis and fermentation under anaerobic conditions [47,49,50], while the presence of Methanosaetaceae (1.26%) suggests limited methanogenic activity.

Genus-level analysis showed similar trends (Figure S3), with greater representation of anaerobic-associated and hydrolytic populations in SBR.M and the ASSR. The community in SBR.M showed intermediate characteristics between the predominantly aerobic community in SBR.C and the anaerobically adapted community in the ASSR, which is consistent with the continuous exchange of sludge between the two reactors. Iron availability may also have influenced microbial metabolism because iron participates in several redox-active cellular processes [51]. However, because microbial communities were only analyzed during the 5 mg Fe/L stage, the effects of iron addition cannot be distinguished from those of anaerobic exposure and reactor history.

The compositional differences were accompanied by differences in PICRUSt2-predicted functional potential inferred from the 16S rRNA gene profiles (Fig. 9b). These predictions represent potential metabolic capabilities rather than direct measurements of pathway activity. The ASSR showed relatively higher contributions of carbohydrate metabolism, energy metabolism, and glycan biosynthesis and metabolism, consistent with a greater potential for processing complex organic substrates under anaerobic conditions [52]. In SBR.M, the relative contributions of amino acid metabolism, protein folding, sorting and degradation, and translation were higher than in SBR.C. The higher predicted amino acid metabolism suggests a greater potential to utilize protein-derived substrates, whereas protein folding, sorting and degradation more likely reflects intracellular protein turnover and cellular adaptation than direct degradation of extracellular or iron-bound proteins [53]. These predicted functions could be compatible with the iron–protein complexation hypothesis if anaerobic exposure in the ASSR increased the availability of protein-derived substrates after the sludge



Fig. 9. Heatmap of (a) microbial community at family level and (b) predicted metabolic pathways in SBR.C, SBR.M, and ASSR.

returned to SBR.M. However, PICRUSt2 cannot determine whether iron–protein complexes were destabilized or whether the predicted functions were actively expressed. Moreover, the limited decrease in organic-N and release of NH_4^+-N within the ASSR do not support extensive protein release and degradation. Therefore, the predicted functional profile provides only indirect evidence of protein-related processing during cyclic anaerobic–aerobic exposure and does not establish iron–protein complex destabilization as the dominant mechanism of sludge reduction.

3.6. Mechanistic synthesis of lower sludge production in the integrated SBR–ASSR system

Lower sludge production in ASSR-based systems is generally attributed to multiple interacting physicochemical and biological processes rather than to a single dominant mechanism. Therefore, this study evaluated three proposed mechanisms: direct sludge degradation within the ASSR, iron-mediated transformation of proteins and organic matter, and altered microbial carbon utilization under cyclic anaerobic–aerobic exposure [6,15,37]. These mechanisms were assessed using physicochemical characterization, mass balances, physiological measurements, and microbial community analysis.

The mass balance results did not support direct sludge degradation within the ASSR as the dominant mechanism. The COD, nitrogen, and VSS mass balances showed that only a limited fraction of the overall decrease in observed sludge production could be attributed to net solids loss within the ASSR. Most of the lower sludge production was therefore associated with reduced net solids formation in SBR.M rather than extensive degradation in the side-stream reactor. At 5 mg Fe/L, the limited COD and organic-nitrogen transformation within the ASSR indicated that anaerobic sludge degradation was not the principal mechanism under this condition.

The results also did not support iron-mediated protein and organic-matter transformation as the dominant explanation. Previous studies on the Cannibal process [13] proposed that under aerobic conditions, iron can interact with proteins and humic substances to form iron–organic matter complexes. Under subsequent anaerobic conditions, destabilization of these complexes may increase substrate availability and contribute to lower sludge production. However, the present results do not support this mechanism as the dominant explanation for sludge reduction in the integrated system. Increasing iron dosage increased observed sludge yield in both SBR.C and SBR.M, while the relative decrease in sludge production remained nearly constant. Thus, although iron affected sludge physicochemical properties and organic matter retention, iron–organic matter complexation was insufficient to explain the lower sludge production in the integrated system.

Among the evaluated mechanisms, the results most consistently supported altered carbon utilization and physiological adaptation associated with cyclic anaerobic–aerobic exposure. Compared with sludge from SBR.C, sludge from SBR.M showed a lower apparent biomass yield despite faster initial substrate uptake. The storage polymer profiles further showed that the additional substrate uptake was not retained as persistent PHA or glycogen, while the lower substrate-induced respiratory response indicated that it was also not associated with immediate aerobic oxidation. The relatively high ATP content and elevated SOD activity were consistent with maintenance of the intracellular energy pool alongside a stronger cellular stress response. Collectively, these observations indicate altered coupling among substrate uptake, storage turnover, respiration, energy conservation, and biomass synthesis. They do not demonstrate classical metabolic uncoupling or increased maintenance metabolism, although greater energy requirements for redox regulation, cellular protection, and recovery may have contributed to non-growth-associated substrate utilization.

This interpretation is also consistent with previous studies showing that ASSR performance strongly depends on operational parameters such as SRT, SIR, and anaerobic exposure conditions [7]. These parameters determine the intensity and duration of the physiological stress imposed during cyclic redox exposure. Lower sludge production may therefore occur within an operational window in which the exposure is sufficient to reduce biomass yield without substantially impairing microbial activity and treatment performance. The operating conditions applied in the present study may fall within such an operational window, although this could not be confirmed because SRT, SIR, and anaerobic exposure time were not systematically varied.

The remaining mechanistic uncertainty is whether the lower apparent biomass yield was primarily due to an increased maintenance-related substrate demand or a lower true growth efficiency, beyond the increased net decay associated with the prolonged SRT in the SBR.M-ASSR system. Future research should therefore determine the specific substrate consumption and biomass growth rates of SBR.C and SBR.M sludge under several controlled growth-rate conditions and analyze them using the Pirt relationship [54]. Comparing the resulting maintenance coefficient and true growth yield would help determine whether the lower apparent yield in SBR.M was primarily associated with greater maintenance requirements or with less efficient coupling between substrate utilization and biomass synthesis.

4. Conclusion

This study evaluated the role of iron dosing and the mechanisms governing lower sludge production in an integrated SBR–ASSR system. Increasing the iron dose increased the observed sludge yield in both SBR.C and SBR.M and enhanced the retention of organic matter and nutrients within the sludge matrix, while the relative reduction in observed sludge yield remained approximately 47%. Mass balances showed that direct solids degradation within the ASSR accounted for only a limited fraction of the lower sludge production. These findings indicate that iron modified sludge-matrix retention but was not the main mechanism responsible for the lower sludge production in SBR.M. Instead, the combined batch and physiological analyses supported altered carbon utilization under cyclic anaerobic–aerobic exposure, in which substrate uptake was less directly coupled to net biomass formation. Thus, further research should determine whether the lower apparent biomass yield results from increased maintenance-related substrate demand or from a lower true growth efficiency.

Declaration of Generative AI and AI-assisted technologies in the writing process

During the preparation of this work, the author(s) used ChatGPT and Grammarly in order to refine the language. After using this tool/service, the author(s) reviewed and edited the content as needed and take(s) full responsibility for the content of the publication.

CRediT authorship contribution statement

Muhammad Fauzul Imron: Writing – original draft, Visualization, Validation, Methodology, Investigation, Formal analysis, Data curation, Conceptualization. **Lenno van den Berg:** Writing – review & editing, Validation, Supervision, Methodology, Conceptualization. **Alexander Hendriks:** Writing – review & editing, Validation, Supervision, Methodology, Conceptualization. **Ralph E.F. Lindeboom:** Writing – review & editing, Validation, Supervision, Methodology, Conceptualization. **Merle de Kreuk:** Writing – review & editing, Validation, Supervision, Methodology, Funding acquisition, Conceptualization.

Declaration of Competing Interest

The authors declare that they have no known competing financial interests or personal relationships that could have appeared to influence the work reported in this paper.

Acknowledgements

The author would like to thank the Ministry of Finance of the Republic of Indonesia and the Indonesia Endowment Fund for Education (LPDP) for funding the first author's PhD program. The author would also like to thank the Waterkracht collective, including the Waterschap Zuiderzeeland, Waterschap Vallei & Veluwe, Waterschap Rijn en IJssel, Waterschap Vechtstromen, and Waterschap Drents Overijsselse Delta, as well as Haskoning in the Netherlands, for supporting this research. The first author would also like to thank Soheil Hadisi and Atharva for helping to operate the reactor during this experiment, and Linghang Li for assisting the first author with measuring PHA.

Appendix A. Supporting information

Supplementary data associated with this article can be found in the online version at doi:10.1016/j.jece.2026.124966.

Data availability

Data will be made available on request.

References

[1] R. Ferrentino, M. Langone, L. Fiori, G. Andreottola, Full-scale sewage sludge reduction technologies: a review with a focus on energy consumption, Water 15 (2023) 615, https://doi.org/10.3390/w15040615.
[2] R. Morello, F. Di Capua, G. Esposito, F. Pirozzi, U. Fratino, D. Spasiano, Sludge minimization in mainstream wastewater treatment: mechanisms, strategies, technologies, and current development, J. Environ. Manag. 319 (2022) 115756, https://doi.org/10.1016/j.jenvman.2022.115756.
[3] S.F. Corsino, D. Di Trapani, F. De Marines, M. Torregrossa, G. Viviani, Influence of the oxic-settling-anaerobic (OSA) process on methane production by anaerobic digestion of sewage sludge, Water 15 (2023) 513, https://doi.org/10.3390/w15030513.
[4] L.P. Sun, Y.J. Lin, C.Y. Shi, S.Q. Wang, W.X. Luo, M. Wang, Effects of interchange ratio on sludge reduction and microbial community structures in an anaerobic/anoxic/oxic process with combined anaerobic side-stream reactor, Water Sci. Technol. 81 (2020) 1250–1263, https://doi.org/10.2166/wst.2020.223.
[5] S. Mulone, S.F. Corsino, M. Capodici, M. Torregrossa, The anaerobic exposure time (AET) as a novel process parameter in the anaerobic side-stream reactor (ASSR)-based process for excess sludge minimization, Water Res. 254 (2024) 121380, https://doi.org/10.1016/j.watres.2024.121380.
[6] G.U. Semblante, F.I. Hai, H.H. Ngo, W. Guo, S.-J. You, W.E. Price, L.D. Nghiem, Sludge cycling between aerobic, anoxic and anaerobic regimes to reduce sludge production during wastewater treatment: performance, mechanisms, and implications, Bioresour. Technol. 155 (2014) 395–409, https://doi.org/10.1016/j.biortech.2014.01.029.
[7] R. Ferrentino, M. Langone, F. Merzari, L. Tramonte, G. Andreottola, A review of anaerobic side-stream reactor for excess sludge reduction: configurations, mechanisms, and efficiency, Crit. Rev. Environ. Sci. Technol. 46 (2016) 382–405, https://doi.org/10.1080/10643389.2015.1096879.
[8] Z. Zhang, Y. Guo, C. Quan, Y. Zhou, Y. Song, J. Li, D. Wang, Tuning phosphorus removal and sludge reduction performance in S2EBPR process by regulating sludge retention time in side-stream anaerobic reactor, J. Water Process. Eng. 70 (2025) 107133, https://doi.org/10.1016/j.jwpe.2025.107133.
[9] K. Li, Y. Wang, Z. Zhang, D. Liu, Effects of oxidation reduction potential in the bypass micro-aerobic sludge zone on sludge reduction for a modified oxic–settling–anaerobic process, Water Sci. Technol. 69 (2014) 2139–2146, https://doi.org/10.2166/wst.2014.135.
[10] N. Di Costanzo, F. Carraturo, M. Salamone, F. Aliberti, S. Masi, D. Caniani, I. M. Mancini, F. Pirozzi, G. Esposito, F. Di Capua, Single-stage C-N-P removal and ultra-low net sludge production driven by cyclic oxygen exposure and side-stream acidogenesis in an intermittent-aeration IFAS-OSA system, Bioresour. Technol. 454 (2026) 134766, https://doi.org/10.1016/j.biortech.2026.134766.
[11] H. Xu, S. Wei, G. Li, B. Guo, Advanced removal of phosphorus from urban sewage using chemical precipitation by Fe-Al composite coagulants, Sci. Rep. 14 (2024) 4918, https://doi.org/10.1038/s41598-024-55713-2.
[12] M.F. Imron, L. van den Berg, A.T.W.M. Hendriks, R.E.F. Lindeboom, M.K. de Kreuk, Iron-mediated protein–humic acid interactions under aerobic and anaerobic conditions: implications for protein hydrolysis and wastewater treatment, Chemosphere 390 (2025) 144718, https://doi.org/10.1016/j.chemosphere.2025.144718.
[13] J.T. Novak, D.H. Chon, B. Curtis, M. Doyle, Biological solids reduction using the cannibal process, Water Environ. Res. 79 (2007) 2380–2386, https://doi.org/10.2175/106143007X183862.
[14] C. Park, M.M. Abu-Orf, J.T. Novak, Predicting the digestibility of waste activated sludges using cation analysis, Proc. Water Environ. Fed. 2003 (2003) 47–69, https://doi.org/10.2175/193864703784755085.
[15] N. Yagci, J.T. Novak, C.W. Randall, D. Orhon, The effect of iron dosing on reducing waste activated sludge in the oxic-settling-anoxic process, Bioresour. Technol. 193 (2015) 213–218, https://doi.org/10.1016/j.biortech.2015.06.109.
[16] G.U. Semblante, F.I. Hai, H. Bustamante, N. Guevara, W.E. Price, L.D. Nghiem, Effects of iron salt addition on biosolids reduction by oxic-settling-anoxic (OSA) process, Int. Biodeterior. Biodegrad. 104 (2015) 391–400, https://doi.org/10.1016/j.ibiod.2015.07.005.
[17] M.F. Imron, L. van den Berg, A. Hendriks, R.E.F. Lindeboom, M. de Kreuk, Insights into sludge reduction in a sequencing batch reactor integrated with an anaerobic side-stream reactor, Process Saf. Environ. Prot. 218 (2026) 109520, https://doi.org/10.1016/j.psep.2026.109520.
[18] J.P. Monteiro, R. Srinivas, L. van den Berg, P. Mirzaee, C. Cruzeiro, M. Alcina Pereira, V.J.P. Vilar, M.K. de Kreuk, J. Pavez-Jara, Mild thermal pre-treatment of waste activated sludge combined with hydrogen peroxide and iron addition, J. Clean. Prod. 568 (2026) 148641, https://doi.org/10.1016/j.jclepro.2026.148641.
[19] A. Gonzalez, J.B. van Lier, M.K. de Kreuk, The role of growth media on composition, bioconversion and susceptibility for mild thermal pre-treatment of waste activated sludge, J. Environ. Manag. 298 (2021) 113491, https://doi.org/10.1016/j.jenvman.2021.113491.
[20] A.H. Nielsen, P. Lens, J. Vollertsen, H. Hvitved-Jacobsen, Sulfide–iron interactions in domestic wastewater from a gravity sewer, Water Res. 39 (2005) 2747–2755, https://doi.org/10.1016/j.watres.2005.04.048.
[21] L.-H. Li, M. Pabst, M.C.M. van Loosdrecht, M. Pronk, Distinct roles of granules and flocs in aerobic granular sludge processes, Water Res. 288 (2026) 124671, https://doi.org/10.1016/j.watres.2025.124671.
[22] A.B. Lanham, A.R. Ricardo, M. Coma, J. Fradinho, M. Carvalheira, A. Oehmen, G. Carvalho, M.A.M. Reis, Optimisation of glycogen quantification in mixed microbial cultures, Bioresour. Technol. 118 (2012) 518–525, https://doi.org/10.1016/j.biortech.2012.05.087.
[23] I. Angelidaki, M. Alves, D. Bolzonella, L. Borzacconi, J.L. Campos, A.J. Guwy, S. Kalyuzhnyi, P. Jenicek, J.B. van Lier, Defining the biomethane potential (BMP) of solid organic wastes and energy crops: a proposed protocol for batch assays, Water Sci. Technol. 59 (2009) 927–934, https://doi.org/10.2166/wst.2009.040.
[24] APHA, Standard methods for examination of water and wastewater, Washing Am. Public. Heal. Assoc. (2012).
[25] M. Dubois, K. Gilles, J.K. Hamilton, P.A. Rebers, F. Smith, A colorimetric method for the determination of sugars, Nature 168 (1951) 167, https://doi.org/10.1038/168167a0.
[26] B. Frølund, T. Griebe, P.H. Nielsen, Enzymatic activity in the activated-sludge floc matrix, Appl. Microbiol. Biotechnol. 43 (1995) 755–761, https://doi.org/10.1007/BF00164784.
[27] A.M. Elgarahy, M.G. Eloffy, A.K. Priya, V. Yogeshwaran, Z. Yang, K.Z. Elwakeel, E. A. Lopez-Maldonado, Biosolids management and utilizations: a review, J. Clean. Prod. 451 (2024) 141974, https://doi.org/10.1016/j.jclepro.2024.141974.
[28] J. Suschka, K. Grübel, Nitrogen in the process of waste activated sludge anaerobic digestion, Arch. Environ. Prot. 40 (2014) 123–136, https://doi.org/10.2478/aep-2014-0021.
[29] W.S. Lee, A.S.M. Chua, H.K. Yeoh, G.C. Ngoh, A review of the production and applications of waste-derived volatile fatty acids, Chem. Eng. J. 235 (2014) 83–99, https://doi.org/10.1016/j.cej.2013.09.002.
[30] X. Wang, S. Wang, T. Xue, B. Li, X. Dai, Y. Peng, Treating low carbon/nitrogen (C/N) wastewater in simultaneous nitrification-endogenous denitrification and phosphorous removal (SNDPR) systems by strengthening anaerobic intracellular carbon storage, Water Res. 77 (2015) 191–200, https://doi.org/10.1016/j.watres.2015.03.019.
[31] Z. Bi, J. Wu, Y. Huang, Y. Pan, Influence of dissolved oxygen on phosphorus removal by polyphosphate-accumulating organisms biofilm: performance and metabolic response, Biochem. Eng. J. 199 (2023) 109048, https://doi.org/10.1016/j.bej.2023.109048.
[32] R. Li, X. Guo, B. Li, L. Lin, P. Li, L. Wen, J. Liang, X. Li, Iron-enhanced primary sedimentation and acidogenic sludge fermentation to achieve self-sufficient organic carbon supply for enhanced nutrient removal in wastewater treatment☆, Resour. Conserv. Recycl. 164 (2021) 105220 https://doi.org/10.1016/j.resconrec.2020.105220.
[33] J. He, X. Zou, P. Zhang, Y. Zhong, X. Pan, J. Zhang, X. Wu, B. Li, X. Tang, X. Xiao, Metal ions-induced structural modification of extracellular polymers: impact of the valence on sludge biodegradability and dewaterability, Int. Biodeterior. Biodegrad. 174 (2022) 105489, https://doi.org/10.1016/j.ibiod.2022.105489.
[34] E. Di Iorio, L. Circelli, R. Angelico, J. Torrent, W. Tan, C. Colombo, Environmental implications of interaction between humic substances and iron oxide nanoparticles: a review, Chemosphere 303 (2022) 135172, https://doi.org/10.1016/j.chemosphere.2022.135172.
[35] H. Deng, J. Yang, R. Li, K. Li, H. Lu, B. Lin, X. Xu, J. Liao, C. Ye, J. Deng, B. Wu, L. Sun, ASSR-mediated sludge yield reduction couples deterministic enrichment of Nitrospira with metabolic resource partitioning, Water Res. 290 (2026) 125031, https://doi.org/10.1016/j.watres.2025.125031.
[36] C. Cheng, J. Geng, H. Hu, Y. Shi, R. Gao, X. Wang, H. Ren, In-situ sludge reduction performance and mechanism in an anoxic/aerobic process coupled with alternating aerobic/anaerobic side-stream reactor, Sci. Total. Environ. 777 (2021) 145856, https://doi.org/10.1016/j.scitotenv.2021.145856.
[37] S.F. Corsino, M. Carabillò, A. Cosenza, F. De Marines, D. Di Trapani, F. Traina, M. Torregrossa, G. Viviani, Insights on mechanisms of excess sludge minimization in an oxic-settling-anaerobic process under different operating conditions and plant configurations, Chemosphere 312 (2023) 137090, https://doi.org/10.1016/j.chemosphere.2022.137090.

[38] M.C.M. Van Loosdrecht, M.A. Pot, J.J. Heijnen, Importance of bacterial storage polymers in bioprocesses, Water Sci. Technol. 35 (1997), https://doi.org/10.1016/S0273-1223(96)00877-3.
[39] F. Carta, J. Beun, M.C. van Loosdrecht, J. Heijnen, Simultaneous storage and degradation of phb and glycogen in activated sludge cultures, Water Res. 35 (2001) 2693–2701, https://doi.org/10.1016/S0043-1354(00)00563-7.
[40] S.-M. Peng, H.-C. Luo, Z.-H. Wang, S.-S. Yang, W.-Q. Guo, N.-Q. Ren, Enhanced in-situ sludge reduction of the side-stream process via employing micro-aerobic approach in both mainstream and side-stream, Bioresour. Technol. 377 (2023) 128914, https://doi.org/10.1016/j.biortech.2023.128914.
[41] J.-S. Guo, F. Fang, P. Yan, Y.-P. Chen, Sludge reduction based on microbial metabolism for sustainable wastewater treatment, Bioresour. Technol. 297 (2020) 122506, https://doi.org/10.1016/j.biortech.2019.122506.
[42] P. Chudoba, J.J. Chevalier, J. Chang, B. Capdeville, Effect of anaerobic stabilization of activated sludge on its production under batch conditions at various So/Xo ratios, Water Sci. Technol. 23 (1991) 917–926, https://doi.org/10.2166/wst.1991.0543.
[43] X. Liu, D. Huang, C. Zhu, F. Zhu, X. Zhu, D. Zhou, Production of reactive oxygen species during redox manipulation and its potential impacts on activated sludge wastewater treatment processes, Environ. Sci. Technol. 58 (2024) 23042–23052, https://doi.org/10.1021/acs.est.4c11301.
[44] Z. Wang, W. Li, H. Li, W. Zheng, F. Guo, Phylogenomics of rhodocyclales and its distribution in wastewater treatment systems, Sci. Rep. 10 (2020) 3883, https://doi.org/10.1038/s41598-020-60723-x.
[45] L. Zhang, X. Huang, J. Zhou, F. Ju, Active predation, phylogenetic diversity, and global prevalence of myxobacteria in wastewater treatment plants, ISME J. 17 (2023) 671–681, https://doi.org/10.1038/s41396-023-01378-0.
[46] I. Mujakić, K. Piwosz, M. Koblížek, Phylum gemmatimonadota and its role in the environment, Microorganisms 10 (2022) 151, https://doi.org/10.3390/microorganisms10010151.
[47] Z. Kondrotaite, L.C. Valk, F. Petriglieri, C. Singleton, M. Nierychlo, M.K. D. Dueholm, P.H. Nielsen, Diversity and ecophysiology of the genus OLB8 and other abundant uncultured saprospiraceae genera in global wastewater treatment systems, Front. Microbiol. 13 (2022) 2229–2238, https://doi.org/10.3389/fmicb.2022.917553.
[48] S.J. McIlroy, P.H. Nielsen, The Family Saprospiraceae. in: The Prokaryotes, Springer Berlin Heidelberg, Berlin, Heidelberg, 2014, pp. 863–889, https://doi.org/10.1007/978-3-642-38954-2_138.
[49] M. Zhu, J. Wang, D. Pei, J. Sun, Y. Lu, Z. Hu, S. Chen, N. Li, The performance and microbial community of anaerobic membrane bioreactor for high calcium papermaking wastewater treatment, J. Water Process. Eng. 56 (2023) 104311, https://doi.org/10.1016/j.jwpe.2023.104311.
[50] S. Hanada, Y. Sekiguchi, The Phylum Gemmatimonadetes. in: The Prokaryotes, Springer Berlin Heidelberg, Berlin, Heidelberg, 2014, pp. 677–681, https://doi.org/10.1007/978-3-642-38954-2_164.
[51] M.R. Teh, A.E. Armitage, H. Drakesmith, Why cells need iron: a compendium of iron utilisation, Trends Endocrinol. Metab. 35 (2024) 1026–1049, https://doi.org/10.1016/j.tem.2024.04.015.
[52] J. Cao, C. Zhang, X. Li, X. Wang, X. Dai, Y. Xu, Microbial community and metabolic pathways in anaerobic digestion of organic solid wastes: progress, challenges and prospects, Fermentation 11 (2025) 457, https://doi.org/10.3390/fermentation11080457.
[53] O.F. Kuzu, L.J.T. Granerud, F. Saatcioglu, Navigating the landscape of protein folding and proteostasis: from molecular chaperones to therapeutic innovations, Signal. Transduct. Target. Ther. 10 (2025) 358, https://doi.org/10.1038/s41392-025-02439-w.
[54] S.J. Pirt, The maintenance energy of bacteria in growing cultures, Proc. R. Soc. Lond. Ser. B. Biol. Sci. 163 (1965) 224–231, https://doi.org/10.1098/rspb.1965.0069.